Volume exclusion effects in perovskite charge transport modeling

Dilara Abdel*, Nicola Courtier†, Patricio Farrell*
* Weierstrass Institute (WIAS), Mohrenstr. 39, 10117 Berlin, Germany
† University of Oxford, Engineering Science, Oxford OX1 3PJ, UK
Email: dilara.abdel@wias-berlin.de

***Abstract*—Due to its flexibility, perovskite materials are a promising candidate for many semiconductor devices. For example, Perovskite Solar Cells (PSCs) have become recently one of the fastest growing photovoltaic technologies [1]. In this work, we take volume exclusion effects into account by formulating two different current densities – either treating the mobility or the diffusion as density dependent while the other quantity remains constant. Finally, we compare both fluxes within drift-diffusion simulations performed by two different open-source tools.**

I. Model Equations

Let α denote a charge carrier (electrons n, holes p or anion vacancies a), n_α be the corresponding density and ψ the electric potential. In perovskites, the carriers' movement is described by a system of partial differential equations [2], [3]

$$-\nabla \cdot (\varepsilon_s \nabla \psi) = q \sum_\alpha z_\alpha (n_\alpha - C_\alpha), \tag{1a}$$

$$z_\alpha q \partial_t n_\alpha + \nabla \cdot \mathbf{j}_\alpha = z_\alpha q r_\alpha, \tag{1b}$$

in an open subdomain $\mathbf{\Omega}_k \subset \mathbf{\Omega} \subset \mathbb{R}^d$, $d \in \{1,2,3\}$, $\mathbf{\Omega} = \cup_k \mathbf{\Omega}_k$. Here, ε_s denotes the relative permittivity, q the elementary charge and z_α the charge number. The doping and the mean ion concentration are given by C_α, a reaction/generation mechanism may be described by r_α and, finally, the motion of charge carriers is described by the current density $\mathbf{j}_\alpha$. The model is supplemented with suitable initial and boundary conditions. We consider a three layer device with an active perovskite layer sandwiched between two doped non-perovskite semiconductor transport layers. Note that the set of unknowns can be given either in terms of the electric potential ψ and the densities of moving carriers n_α, $\alpha = n, p, a$, or in terms of $(\psi, \varphi_n, \varphi_p, \varphi_a)$, where φ_α denote the respective quasi Fermi potentials. These potentials are linked to the charge carrier densities via (for $\alpha = n, p, a$)

$$n_\alpha = N_\alpha \mathcal{F}_\alpha\Big(\eta_\alpha(\psi, \varphi_\alpha)\Big),\ \eta_\alpha = z_\alpha \frac{q(\varphi_\alpha - \psi) + E_\alpha}{k_B T}, \tag{2}$$

where N_n, N_p are the effective density of states and E_n, E_p the conduction and valence band-edge energies. Further, N_a is the maximum ion vacancy concentration and E_a the formation energy. The parameter k_B refers to the Boltzmann constant and T to the temperature. We call $\mathcal{F}_\alpha$ statistics function, which for non-degenerate semiconductors is an exponential. To include volume exclusion effects we define $\mathcal{F}_a(\eta) = (\exp(-\eta)+1)^{-1}$.

II. Current density descriptions

The perovskite model (1) is supplemented with following current density descriptions for electrons and holes

$$\mathbf{j}_n = -q z_n \left(D_n \nabla n_n + z_n \mu_n n_n \nabla \psi\right), \tag{3a}$$

$$\mathbf{j}_p = -q z_p \left(D_p \nabla n_p + z_p \mu_p n_p \nabla \psi\right), \tag{3b}$$

where the diffusion coefficient D_α and the mobility μ_α, $\alpha = n, p$, are related via the generalized Einstein relation [2]

$$D_\alpha = \mu_\alpha U_T g_\alpha\left(\frac{n_\alpha}{N_\alpha}\right),\ g_\alpha\left(\frac{n_\alpha}{N_\alpha}\right) = \frac{n_\alpha}{N_\alpha}(\mathcal{F}_\alpha^{-1})'\left(\frac{n_\alpha}{N_\alpha}\right), \tag{4}$$

where U_T is the thermal voltage and g_α the diffusion enhancement. For non-degenerate semiconductors we have $g_n = g_p = 1$ with constant mobilities and diffusion coefficients. To limit ionic depletion, we need to incorporate volume exclusion effects into the current density expression of anion vacancies $\mathbf{j}_\alpha$. On the one hand, assuming a constant mobility $\mu_a = \overline{\mu}_a$ and applying (4) the current density comprises nonlinear diffusion [2]

$$\mathbf{j}_{a,1} = -q z_a \overline{\mu}_a U_T \left(g_a\left(\frac{n_a}{N_a}\right)\nabla n_a + \frac{z_a}{U_T} n_a \nabla \psi\right), \tag{5}$$

where $g_a = (1 - n_a/N_a)^{-1}$. On the other hand, a constant diffusion coefficient $D_a = \overline{D}_a$, called the tracer diffusivity, allows us to express the mobility in terms of an activity coefficient, which is given by the diffusion enhancement g_a for diffusion on a lattice [4]. This leads to a current density expression with a modified drift term

$$\mathbf{j}_{a,2} = -q z_a \overline{D}_a \left(\nabla n_a + \frac{z_a}{U_T g_a\left(\frac{n_a}{N_a}\right)} n_a \nabla \psi\right). \tag{6}$$

III. Current density discretizations

We will discretize the perovskite model (1) for both fluxes (5) and (6) via two different simulation tools/techniques. While `ChargeTransport.jl` uses a finite volume method (FVM), `IonMonger` is based on the finite element method (FEM), see [3], [5], [6] for further information. Next, we introduce the local FVM and FEM flux discretizations for (5) and (6). Let the subindices K and L denote the evaluation of a quantity at the neighboring nodes $\mathbf{x}_K$ and $\mathbf{x}_L$, respectively,

978-1-6654-7899-1/22/$31.00 ©2022 IEEE

and $\delta\psi = (\psi_L - \psi_K)/U_T$. `IonMonger` uses dimensionless flux approximations equivalent to numerical current densities

$$j^{\mathrm{IM}}_{1,KL} = -q\overline{\mu}_a U_T \left[\frac{L(n_{a,L}) - L(n_{a,K})}{h_{KL}} + \bar{n}_2 \frac{\delta\psi}{h_{KL}}\right],$$
$$j^{\mathrm{IM}}_{2,KL} = -q\overline{D}_a \left[\frac{n_{a,L} - n_{a,K}}{h_{KL}} + (\bar{n}_2 - \bar{n}_3)\frac{\delta\psi}{h_{KL}}\right],$$

where $L(n) = N_a \log\left(1 - \frac{n}{N_a}\right)$ and h_{KL} denotes the Euclidean distance between $\mathbf{x}_K$ and $\mathbf{x}_L$. Moreover, we used the averaged densities $\bar{n}_2 = \frac{1}{2}(n_{a,L} + n_{a,K})$ and $\bar{n}_3 = \frac{1}{3N_a}(n_{a,L}^2 + n_{a,L}n_{a,K} + n_{a,K}^2)$. In `ChargeTransport.jl` the modified Scharfetter-Gummel fluxes are implemented as

$$j^{\mathrm{CT}}_{1,KL} = \frac{q\overline{\mu}_a U_T \bar{g}_{KL}}{h_{KL}} \left(B\left(\frac{\delta\psi}{\bar{g}_{KL}}\right) n_{a,K} - B\left(\frac{-\delta\psi}{\bar{g}_{KL}}\right) n_{a,L}\right),$$
$$j^{\mathrm{CT}}_{2,KL} = \frac{q\overline{D}_a}{h_{KL}} \left(B\left(\frac{\delta\psi}{\bar{g}_{KL}}\right) n_{a,K} - B\left(\frac{-\delta\psi}{\bar{g}_{KL}}\right) n_{a,L}\right).$$

Here, B denotes the Bernoulli function given as $B(x) = x/\left(\exp(x) - 1\right), B(0) = 1$. The only choice of $\bar{g}_{KL}$ consistent with thermodynamic equilibrium [7] is

$$\bar{g}_{KL} = \frac{\eta_{a,L} - \eta_{a,K}}{\log \mathcal{F}(\eta_{a,L}) - \log \mathcal{F}(\eta_{a,K})},$$

where $\eta_{a,K}, \eta_{a,L}$ are evaluations of the argument of $\mathcal{F}_a$ in (2).

IV. Numerical simulation

Using the parameter template of [3], a PSC three layer device based on the two alternative current density descriptions was simulated for a linear IV scan protocol with a scan rate $0.04\,\mathrm{V/s}$ with both software tools. For simplicity, surface effects are neglected. We denote the ratio between the maximum vacancy concentration N_a and the average vacancy concentration C_a by ϵ. The evolution of the electric potential ψ is depicted in Figure 1 for a case of low ($\epsilon = 0.01$) and high ($\epsilon = 0.95$) volume exclusion effects. The colored lines correspond to a solution calculated with `IonMonger` whereas the black dotted lines indicate respective solutions calculated with `ChargeTransport.jl`. Brighter color indicates later time. First, we notice that both software tools yield the same results. Second, for high volume exclusion (larger ϵ) the modified drift in (6) causes a slower evolution of the ion profile (shown by the potential gradients remaining large) compared to the flux with nonlinear diffusion (5). In fact, this can be also observed in the ion vacancy density profiles in Figure 2.

V. Summary and Outlook

For a PSC model, we discussed two types of continuous current densities: nonlinear diffusion (5) and modified drift (6). We discretized both fluxes via two different methods (FVM and FEM) and showed in simulations that both discretizations yield the same result: The modified drift current leads to an ion profile which changes more slowly compared to the current density with nonlinear diffusion. The effect on the ion distribution near an interface was also demonstrated.

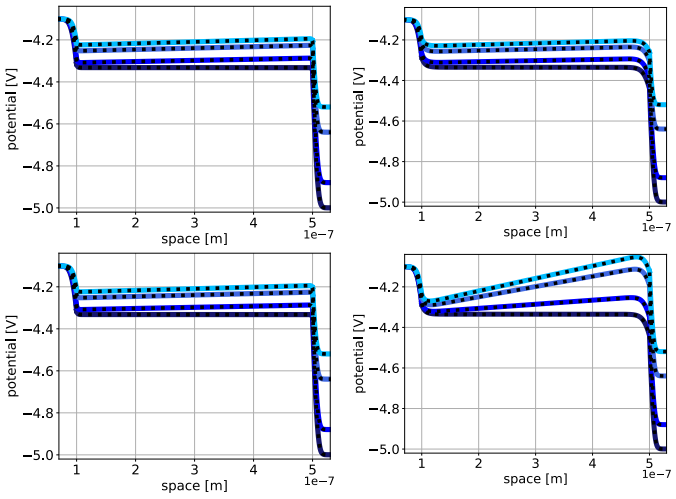

Fig. 1. Evolution of the electric potential ψ solving the model (1) based on the nonlinear diffusion current (5) (first row) and for the model based on the modified drift current (6) (second row). The first column shows the case of $\epsilon = 0.01$ for $E_a = -4.45$eV (low exclusion) and the second column of $\epsilon = 0.95$ for $E_a = -4.26$eV (high exclusion). Brighter colors indicate later time.

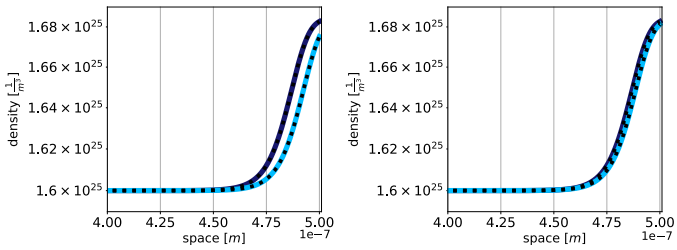

Fig. 2. Evolution of the vacancy density n_a at the right perovskite/hole transport layer interface based on the nonlinear diffusion current (5) (left) and for the modified drift current (6) (right) for $\epsilon = 0.95$. The second current leads to a slower evolution of the ion profile. Given sufficient relaxation time, the two descriptions result in the same equilibrium profile.

References

[1] N. Tessler and Y. Vaynzof, "Insights from device modeling of perovskite solar cells", *ACS Energy Letters* **5** (4) (2020), 1260—1270.

[2] D. Abdel, P. Vagner, J. Fuhrmann and P. Farrell, "Modelling charge transport in perovskite solar cells: Potential-based and limiting ion depletion", *Electrochimica Acta*, vol. 390, pp. 138696, 2021.

[3] N. E. Courtier, J. M. Cave, A. B. Walker, G. Richardson and J. M. Foster, "IonMonger: a free and fast planar perovskite solar cell simulator with coupled ion vacancy and charge carrier dynamics", *Journal of Computational Electronics*, vol. 18, pp. 1435–1449, 2019.

[4] M. Bazant, "Theory of Chemical Kinetics and Charge Transfer based on Nonequilibrium Thermodynamics", *Accounts of Chemical Research*, vol. 46, pp. 1144–1160, 2013.

[5] D. Abdel, P. Farrell and J. Fuhrmann, "ChargeTransport.jl: Simulating charge transport in semiconductors", doi: 10.5281/zenodo.6275688, 2022.

[6] N. E. Courtier, G. Richardson and J. M. Foster, "A fast and robust numerical scheme for solving models of charge carrier transport and ion vacancy motion in perovskite solar cells", *Applied Mathematical Modelling*, vol. 63, pp. 329–348, 2018.

[7] M. Bessemoulin-Chatard, "A finite volume scheme for convection–diffusion equations with nonlinear diffusion derived from the Scharfetter–Gummel scheme", *Numerische Mathematik*, vol. 121, pp. 637–670, 2012.